Mon. Not. R. Astron. Soc. **000**, 1–8 (1999) Printed 30 August 2018 (MN LaTeX style file v1.4)

Radial velocity measurements of white dwarfs

P. F. L. Maxted, T. R. Marsh, C. K. J. Moran,
University of Southampton, Department of Physics & Astronomy, Highfield, Southampton, S017 1BJ, UK

Accepted 1999 Received 1999

ABSTRACT

We present 594 radial velocity measurements for 71 white dwarfs obtained during our search for binary white dwarfs and not reported elsewhere. We identify three excellent candidate binaries, which require further observations to confirm our preliminary estimates for their orbital periods, and one other good candidate. We investigate whether our data support the existence of a population of single, low mass ($\lesssim 0.5 M_{\odot}$) white dwarfs (LMWDs). These stars are difficult to explain in standard models of stellar evolution. We find that a model with a mixed single/binary population is at least ~ 20 times more likely to explain our data than a pure binary population. This result depends on assumed period distributions for binary LMWDs, assumed companion masses and several other factors. Therefore, the evidence in favour of the existence of a population of single LMWDs is not sufficient, in our opinion, to firmly establish the existence of such a population, but does suggest that extended observations of LMWDs to obtain a more convincing result would be worthwhile .

Key words: white dwarfs – binaries: close – binaries: spectroscopic

1 INTRODUCTION

The observed mass distribution of white dwarf stars is strongly peaked around $0.55 M_{\odot}$ (Finley et al. 1997, Bergeron et al. 1992, Bragaglia et al. 1995). Although models of the evolution leading to white dwarfs are extremely uncertain, it appears that this is the minimum mass of a white dwarf that can be formed through single star evolution in the lifetime of the Galaxy (Bragaglia et al. 1995). White dwarfs more massive than this minimum are formed from initially more massive stars, but they are much less common than lower mass stars, and so the observed mass distribution is strongly peaked. In this paper we deal with white dwarf stars below this "minimum" mass. These are thought to be the result of binary star evolution, in which the evolution of a star during the red giant phase is interrupted by interactions with a nearby star. The physics of this interaction is complex but it is thought to lead to the stripping of the outer hydrogen layers from the red giant in a "common-envelope" phase, halting the formation of the degenerate helium core and leading to the formation of an anomalously low mass white dwarf (Iben & Livio 1993). The hypothesis that binary evolution forms low mass white dwarfs (LMWDs) was confirmed by the discovery of Marsh et al. (1995) of at least 5 short period binary white dwarfs in a sample of 7 LMWDs. However, there is growing evidence that LMWDs may not all be binaries (Maxted & Marsh 1998). It has been suggested that this is a result of the merging of the binary following the common-envelope phase (Iben et al. 1997), but the lack of any detectable rotation in the apparently single white dwarfs has cast doubt on this suggestion (Maxted & Marsh 1998). An alternative hypothesis is that the giant planets recently discovered orbiting solar-type stars lead to a common-envelope phase, but evaporate during that phase leaving an apparently single LMWD (Nelemans & Tauris 1998).

We have been successful in finding new white dwarf binaries and measuring their orbital periods using the techniques of Marsh et al. (1995). Those results have been presented elsewhere (Moran 1999; Moran, Marsh & Maxted 2000; Maxted , Marsh & Moran, 2000). We have observed many white dwarfs in the course of our search for binary white dwarfs but have not, in general, reported these radial velocity measurements unless the star was found to be a binary and the orbital period identified. These radial velocity measurements are a valuable resource, both for kinematic studies and for future surveys for binary white dwarfs. Therefore, in this paper we report our 594 radial velocity measurements for 71 white dwarfs not already reported elsewhere. We identify 4 new candidate binary white dwarfs and report preliminary orbital periods for three of them. We also consider the evidence for the existence of a population of single low mass white dwarfs.

2 OBSERVATIONS AND REDUCTIONS

The data have been obtained over several years using several instruments. Most of the data come from observations obtained with the intermediate dispersion spectrograph (IDS) on the 2.5m Isaac Newton Telescope (INT) on the Island of La Palma. Additional spectra for some stars were obtained using the ISIS spectrograph on the 4.2m William Herschel Telescope (WHT), also on La Palma, and the RGO spectrograph on the 3.9m Anglo-Australian Telescope (AAT) at Siding Spring, Australia. The detectors used in every case were charge-coupled devices (CCDs). Details of all three instruments, the dates of all the observing runs and the dispersion per pixel used are given in Table 1.

The observing procedure is very similar in each case. We obtain spectra of our target stars around the Hα line with a resolution of $\lesssim$1Å. Exposure times are typically 5–20 minutes and never longer than 30 minutes. Spectra of an arc lamp are taken before and after each target spectrum with the telescope tracking the star. None of the CCDs used showed any structure in unexposed images, so a constant bias level determined from a clipped-mean value in the overscan region was subtracted from all the images. Sensitivity variations were removed using observations of a tungsten calibration lamp. The sensitivity variations along the spectrograph slit are removed using observations of the twilight sky in the AAT images because the tungsten calibration lamp is inside the spectrograph. We have occasionally used the same technique for the WHT and INT spectra, though it makes little difference in practice whether we use sky images or lamp images to calibrate these images.

Extraction of the spectra from the images was performed automatically using optimal extraction to maximize the signal-to-noise of the resulting spectra (Horne 1986). The arcs associated with each stellar spectrum were extracted using the profile determined for the stellar image to avoid possible systematic errors due to tilted arc lines. The wavelength scale was determined from a polynomial fit to measured arc line positions and the wavelength of the target spectra interpolated from the calibration established from the bracketing arc spectra. Uncertainties on every data point calculated from photon statistics are rigorously propagated through every stage of the data reduction.

Table 1. Summary of the spectrograph/telescope combinations used to obtain spectra for this study. The slit width used in each case is approximately 1arcsec. The resolution and the sampling are both in units of Å.

Date	Telescope	Spectrograph	Resolution	Sampling
Mar 96	AAT	RGO	0.7	0.23
Aug 97	AAT	RGO	0.7	0.24
Mar 97	AAT	RGO	0.7	0.23
Jun 98	AAT	RGO	0.7	0.29
Mar 99	AAT	RGO	0.7	0.29
Apr 94	INT	IDS	0.7	0.36
Jun 95	INT	IDS	0.9	0.39
Feb 97	INT	IDS	0.9	0.39
Jun 97	INT	IDS	0.9	0.39
Nov 97	INT	IDS	0.9	0.39
Feb 98	INT	IDS	0.9	0.39
Sep 98	INT	IDS	0.9	0.39
Feb 99	INT	IDS	0.9	0.39
Apr 99	INT	IDS	0.6	0.30
Jun 93	WHT	ISIS	0.8	0.38
Aug 93	WHT	ISIS	0.8	0.38
Jul 94	WHT	ISIS	1.8	0.74
Jan 95	WHT	ISIS	0.8	0.40
Nov 97	WHT	ISIS	0.8	0.40
Feb 98	WHT	ISIS	0.8	0.40
Jul 98	WHT	ISIS	0.8	0.40

3 ANALYSIS

3.1 Radial velocity measurements.

To measure the radial velocities we used least-squares fitting of a model line profile. This model line profile is the summation of four Gaussian profiles with different widths and depths but with a common central position which varies between spectra. Only data within 5000 km s^{-1} of the Hα line is included in the fitting process. We first normalize the spectra using a linear fit to the continuum either side of the Hα line. We then use a least-squares fit to all the spectra to establish the shape of the model line profile. A least squares fit of this profile to each spectrum in which the position of the line is the only free parameter gives the final heliocentric radial velocities reported in Table 9. The uncertainties quoted are calculated by propagating the uncertainties on every data point in the spectra right through the data reduction and analysis. These uncertainties are reliable in most cases, but some caution must be exercised for quoted uncertainties of less than ~ 0.5 km s^{-1}. This corresponds to less than 1/20 of a pixel in the original data, so systematic errors such as telluric absorption features and uncertainties in the wavelength calibration are certain to be a significant source of uncertainty for these measurements.

Where data has been obtained for a star on more than one instrument we have measured the offset between the data sets to look for systematic differences. These offsets are given in Table 2. Almost all of these offsets are consisted with an offset between data sets of no more than ~ 1 km s^{-1}. The obvious exceptions are WD 0341+021 and WD 1407−475, which we discuss more fully below.

3.2 Criterion for variability.

For each star we calculate a weighted mean radial velocity. This mean is the best estimate of the radial velocity of the star assuming this quantity is constant. We then calculate the χ^2 statistic for this “model”, i.e. the goodness-of-fit of a constant to the observed radial velocities. We can then compare the observed value of χ^2 with the distribution of χ^2 for the appropriate number of degrees of freedom. We then calculate the probability of obtaining the observed value of χ^2 or higher from random fluctuations of constant value, p. The observed values of the weighted mean radial velocity, χ^2 and the logarithm of this probability, $\log_{10}(p)$, are given for all the white dwarfs in our sample in Table 4. If we find $\log_{10}(p) < -4$ we consider this to be a detection of a binary. In a sample of 71 objects, this results in a less than 1 percent chance of random fluctuations producing one or more false detections.

In order to estimate the fraction of binaries that would be detected using our observations with this detection criterion we use a Monte Carlo approach. We generate synthetic radial velocity measurements with the same temporal sampling and accuracy as the actual observations of each star and add the appropriate amount of noise. We include the

Table 2. Measurements of offsets in radial velocity measurements between various data sets.

Star	First observing run	Second observing run	Offset ($\mathrm{km\,s^{-1}}$)
WD 0132+254	WHT, Nov 97	INT, Feb 98	$+6.9 \pm 4.0$
WD 0316+345	WHT, Jan 95	INT, Sep 98	-0.5 ± 1.6
WD 0341+021	WHT, Nov 97	INT, Feb 98	-31.5 ± 6.9
WD 0401+250	INT, Nov 97	INT, Feb 98	$+1.6 \pm 2.7$
WD 0401+250	WHT, Nov 97	INT, Feb 98	-1.9 ± 2.7
WD 0437+152	WHT, Nov 97	INT, Feb 98	-0.9 ± 3.0
WD 0453+418	WHT, Jan 95	INT, Feb 99	-3.4 ± 1.2
WD 0549+158	INT, Feb 98	INT, Feb 99	-1.9 ± 3.0
WD 0808+595	WHT, Nov 97	INT, Feb 98	-2.6 ± 6.5
WD 1031−114	INT, Feb 99	AAT, Mar 99	-3.4 ± 2.7
WD 1105−048	AAT, Mar 97	INT, Feb 99	$+0.3 \pm 1.2$
WD 1105−048	AAT, Mar 96	INT, Feb 99	$+0.5 \pm 0.7$
WD 1257+032	WHT, Jan 95	INT, Jun 95	$+3.2 \pm 2.5$
WD 1257+032	INT, Jun 95	AAT, Mar 99	-0.9 ± 5.6
WD 1257+032	WHT, Jan 95	AAT, Mar 99	$+2.3 \pm 5.7$
WD 1310+583	INT, Jul 97	INT, Feb 98	$+1.2 \pm 2.2$
WD 1327−083	AAT, Mar 97	AAT, Jun 98	-1.3 ± 0.3
WD 1327−083	AAT, Mar 96	AAT, Jun 98	$+1.1 \pm 0.2$
WD 1353+409	WHT, Jun 93	WHT, Jan 95	-3.8 ± 3.5
WD 1353+409	WHT, Jan 95	WHT, Feb 98	$+9.3 \pm 3.2$
WD 1407−475	AAT, Mar 96	AAT, Mar 97	-22.0 ± 1.5
WD 1614+136	WHT, Jun 93	WHT, Feb 98	$+2.1 \pm 2.1$
WD 1614+136	WHT, Jun 93	AAT, Jun 96	$+1.9 \pm 4.7$
WD 1620−391	AAT, Mar 97	AAT, Aug 97	$+3.6 \pm 0.6$
WD 1620−391	AAT, Mar 97	AAT, Jun 98	-0.8 ± 1.6
HS 1653+7753	INT, Sep 98	INT, Feb 99	-3.0 ± 8.2
WD 1943+163	INT, Jun 95	AAT, Jun 95	$+0.8 \pm 2.1$

projection effects due to randomly oriented orbits. Periods are selected randomly from one of the theoretical period distributions described below. The mass of the white dwarf observed, M, is taken from Table 4 if known or is calculated for each trial perid P from $\log(M) = 0.13\log(P) - 0.6$. This is simply an approximation to the main feature of the bivariate distribution of periods and masses for binary white dwarfs given by Saffer et al. (1998). We then estimate our detection efficiency using the number of trials which statisfy our detection criterion for the following two cases.

The first case is a white dwarf companion with the same mass as the visible white dwarf. We use the sum of the period distributions for white dwarfs with white dwarf companions of all types including the loss of systems due to 10^8y of gravitational wave radiation given by Iben et al. (1997, their Figs 2(c) and 2(d)). Note that their models give a mean mass ratio of around 0.7 with the fainter, i.e., older, companion being more massive. However, there are now six white dwarf – white dwarf binaries with directly measured mass ratios, and these tend to be $\gtrsim 1$ (Table 3). It is not straightforward to estimate the selection effects but a mass ratio of 1 does seem to be more typical for these binaries. This detection efficiency is given in Table 4 under $e(A)$.

The second case is a main-sequence companion with a mass of $0.08\mathrm{M}_\odot$. The theoretical period distribution in this case is the sum of the distributions given by Iben et al. for companions to white dwarfs with mass less than $0.3\mathrm{M}_\odot$ (their Figs 3(c) and 3(d)). This detection efficiency is given in Table 4 under $e(B)$. We use 100,000 trials to measure these efficiencies, which is sufficient to give an accuracy of a few tenths of one percent. We can also plot these detection efficiencies as a function of period to get a more qualitative view. Some examples are shown in Fig. 1.

Table 3. Measured mass ratios for white dwarf – white dwarf binaries.

Name	Mass ratio	Reference
WD 0136+768	1.27±0.04	Moran, Maxted & Marsh 2000
WD 0135-052	0.90±0.04	Saffer et al. 1988
WD 0957−666	1.14±0.02	Moran, Maxted & Marsh 2000
WD 1101+364	0.87±0.03	Marsh 1995
WD 1204+450	1.095±0.04	Moran, Maxted & Marsh 2000
WD 1704+481.2	0.70±0.03	Maxted, Marsh & Moran 2000

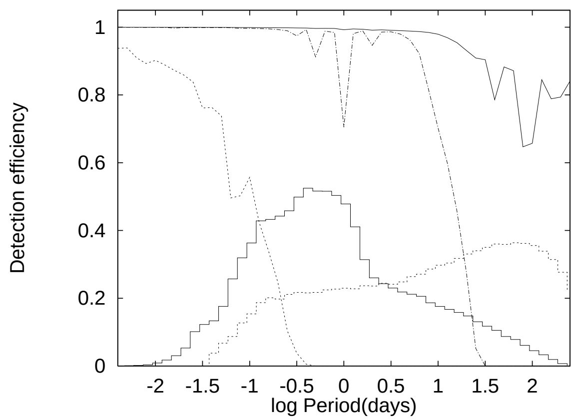

Figure 1. The detection efficiency as a function of orbital period assuming a mass ratio of one for WD 0346−011 (dashed line), WD 0913+442, (dash-dotted line) and WD 0101+048 (solid line). The theoretical period distributions used to estimate the detection efficiencies for stars with white dwarf companions (histogram, solid line) and main sequence companions (histogram, dashed line) are also shown.

4 NOTES ON INDIVIDUAL OBJECTS

WD 0101+048: This object is variable according to our criterion. The Hα line is narrower than usual so we only use data within 2000 $\mathrm{km\,s^{-1}}$ of Hα to measure the radial velocities. The periodogram of these velocities is complex with peaks near 0.16cycles/d and 0.85cycles/d. We used a circular orbit fit by least squares to the measured radial velocities to fix the position of the absorption core in each spectrum in a least-squares fit to all the spectra to re-determine the model line profile. We then re-measured the radial velocities with this improved model line profile. These are the velocities given in Table 9. The periodogram of these data shows many peaks of similar significance. We used the seven most significant peaks to give an initial value of the period in a least-squares fit of a circular orbit to the data. The results are given in Table 5. Periods near 6.4d and 1.2d are equally likely and there are several periods near these values which would give a satisfactory fit to our data. The real period of this binary should be easy to identify with a few more spectra. The value of chi-squared is unusually low for all the circular orbit fits in Table 5. There are 14 data points and 4 free parameters in the fitting process, so we might expect a typical value of chi-squared around 10, but a value of chi-squared as low as 5.27 occurs by chance for about 1/8

Table 4. Summary of our radial velocity measurements for white dwarfs. References for the masses are as follows: 1. Bergeron et al. 1992; 2. Bergeron et al. 1995; 3. Finley et al. 1997; 4. Homeier et al. 1998; 5. Moran 1999; 6. Vennes et al. 1997; 7. Bragaglia et al.1995.

Name	N	Mean ($km\,s^{-1}$)	χ^2	$\log_{10}(p)$	$e(A)$ (%)	e(B) (%)	Mass ($M_\odot$)	Ref.
WD 0011+000	3	27.0 ± 2.3	2.80	-0.61	66.6	21.5		
WD 0101+048	14	63.4 ± 0.2	105.27	-15.80	99.1	68.2		
WD 0126+101	6	7.1 ± 0.4	5.90	-0.50	90.8	40.8	0.50 ±0.03	5
WD 0132+254	8	36.3 ± 0.5	5.71	-0.24	95.5	49.1	0.36 ±0.03	5
WD 0142+312	8	37.6 ± 1.1	11.41	-0.92	86.1	35.7		
WD 0143+216	5	20.8 ± 1.2	7.17	-0.89	82.5	32.2		
WD 0147+674	6	30.2 ± 1.1	9.65	-1.07	79.9	22.6	0.45±0.03,0.48±0.01	1,3
WD 0148+467	2	15.3 ± 2.4	0.44	-0.29	34.3	4.3	0.53±0.03,0.57±0.03	1,5
WD 0151+017	4	63.2 ± 0.8	0.64	-0.05	72.1	21.5	0.48 ±0.03	5
WD 0213+396	6	26.2 ± 1.4	22.36	-3.35	86.5	36.8		
WD 0316+345	12	-42.9 ± 0.2	27.82	-2.46	98.4	64.8	0.40±0.03	1
WD 0320−539	7	57.8 ± 0.8	14.21	-1.56	87.8	30.0	0.58±0.02,0.47±0.03	3,7
WD 0332+320	4	100.9 ± 1.7	2.60	-0.34	66.2	11.8	0.71±0.03	5
WD 0339+523	9	3.3 ± 0.5	7.41	-0.31	92.8	46.5	0.34±0.03	1
WD 0341+021	7	-53.2 ± 0.6	33.65	-5.11	94.1	45.6	0.38±0.03	5
WD 0346−011	10	134.5 ± 5.2	26.95	-2.85	55.2	0.0	1.27±0.03,1.23±0.08	1,4
WD 0401+250	11	81.7 ± 0.3	10.16	-0.37	98.8	49.9	0.63±0.03	5
WD 0407+179	1	62.5± 2.3	—	—	—	—	0.49±0.03	5
WD 0416+334	6	-44.4 ± 0.7	8.79	-0.93	90.7	45.2		
WD 0416+701	18	21.3 ± 0.2	92.48	-11.67	98.7	62.6		
WD 0437+152	8	21.1 ± 0.5	6.32	-0.30	95.5	48.3	0.38±0.03	5
WD 0446−789	7	40.2 ± 0.4	3.24	-0.11	91.5	42.0	0.51±0.02 7 7	
WD 0453+418	15	59.7 ± 0.2	29.83	-2.09	99.0	69.3	0.43±0.03	1
WD 0507+045.1	6	37.8 ± 0.8	6.95	-0.65	90.2	32.3	0.61±0.03	5
WD 0507+045.2	6	48.2 ± 1.5	4.24	-0.29	85.4	15.2	0.71±0.03	5
WD 0509−007	5	22.1 ± 1.5	3.16	-0.27	88.5	36.1	0.382±0.005	3
WD 0516+365	2	54.8 ± 4.6	0.43	-0.29	26.0	1.9	0.59±0.03	5
WD 0549+158	17	30.0 ± 0.6	18.00	-0.49	95.7	38.9	0.47±0.02, 0.51±0.01	4,3
WD 0658+624	6	13.6 ± 0.7	6.33	-0.56	90.7	37.1	0.54±0.03	5
WD 0752−146	4	28.6 ± 1.2	19.19	-3.60	86.1	34.7		
WD 0752−146 B	4	-146.8 ± 1.3	17.58	-3.27	85.3	33.4		
WD 0808+595	7	15.3 ± 1.1	7.62	-0.57	88.9	29.6	0.37±0.03	5
WD 0824+288 B	2	-36.8 ± 2.9	0.02	-0.06	19.3	3.6		
WD 0839+231	8	0.3 ± 0.5	3.72	-0.09	93.0	40.7	0.48±0.03,0.48±0.01	1,3
WD 0906+296	8	93.5 ± 1.0	3.95	-0.11	84.5	23.9	0.52±0.03	5
WD 0913+442	6	58.6 ± 0.7	5.93	-0.50	91.2	33.1	0.76±0.04,0.70±0.03	2,5
WD 0945+245	5	62.7 ± 2.1	2.78	-0.23	82.9	27.1		
WD 0950−572	2	46.2 ± 6.7	0.01	-0.04	27.8	3.3	0.42±0.03	5
WD 0954+247	5	59.9 ± 0.7	6.91	-0.85	85.4	37.3		
WD 0954−710	7	18.6 ± 0.3	16.86	-2.01	95.5	53.8	0.47±0.03,0.45±0.04	5,7
WD 1026+023	8	18.2 ± 0.6	11.05	-0.86	90.7	37.8	0.53±0.03,0.54±0.03	3,5
WD 1029+537	5	35.4 ± 5.6	12.46	-1.85	61.1	1.0	0.58±0.02	3
WD 1031−114	8	41.1 ± 0.9	5.54	-0.23	97.7	48.2	0.52±0.01, 0.57±0.03	3,5
WD 1036+433	5	-5.6 ± 0.4	2.19	-0.15	97.3	64.3		
WD 1039+747	4	47.7 ± 3.8	2.88	-0.39	60.8	6.8	0.45±0.03	1
WD 1105−048	18	50.8 ± 0.1	36.10	-2.35	99.9	88.9	0.49±0.03,0.48±0.03,0.53±0.03	1,4,5
WD 1229−012	9	18.6 ± 1.0	26.10	-3.00	95.4	38.5	0.42 ±0.03	5
WD 1232+479	10	6.0 ± 0.4	17.27	-1.35	91.1	40.1	0.53±0.03	1
WD 1257+032	17	23.8 ± 0.4	25.99	-1.27	97.6	45.6	0.46±0.03	1
WD 1310+583	15	4.5 ± 0.3	8.97	-0.08	97.1	38.6		
WD 1327−083	19	45.1 ± 0.1	82.77	-9.55	100.0	97.1	0.52±0.03,0.50±0.02	5,7
WD 1353+409	13	-2.6 ± 0.5	16.29	-0.75	97.6	47.1	0.40±0.03	1
WD 1407−475	17	38.5 ± 0.2	292.70	< -45	99.2	64.7	0.50±0.02	7
WD 1422+095	6	1.6 ± 0.7	14.85	-1.96	92.1	41.3	0.51±0.04	7
EUVE 1439+750	4	-140.9 ± 10.5	12.20	-2.17	27.7	2.1	0.96±0.05,0.99±0.05	6,6
WD 1507+220	10	-50.7 ± 0.5	6.31	-0.15	93.3	42.2	0.50±0.03	1
WD 1507−105	2	-14.0 ± 5.6	0.00	-0.02	26.9	6.1		

Table 4. continued.

Name	N	Mean (km s^{-1})	χ^2	$\log_{10}(p)$	$e(A)$ (%)	e(B) (%)	Mass (M$_\odot$)	Ref.
WD 1614+136	15	5.2 ± 0.5	25.67	-1.54	98.1	56.5	0.33±0.03	1
WD 1615−157	2	12.8 ± 6.7	0.13	-0.14	26.3	1.7	0.62±0.02,0.66±0.02	3,7
WD 1620−391	11	47.5 ± 0.1	32.44	-3.47	99.5	74.0	0.62±0.01,0.66±0.02	3,7
WD 1637+335	5	27.5 ± 1.0	8.80	-1.18	82.7	34.0		
WD 1647+591	13	41.6 ± 1.1	7.71	-0.09	89.8	41.0		
HS 1653+7753	5	-1.2 ± 2.5	0.96	-0.04	71.6	16.9	0.32±0.02	4
WD 1655+215	5	40.0 ± 1.3	6.48	-0.78	87.2	34.3		
WD 1911+135	10	20.7 ± 0.4	12.23	-0.70	94.0	45.6	0.49±0.03,0.50±0.03	1,2
WD 1943+163	14	36.3 ± 0.4	5.84	-0.02	97.4	50.5	0.49±0.03	1
WD 2058+506	15	8.2 ± 0.5	17.65	-0.65	92.2	44.5		
WD 2111+261	12	-2.4 ± 0.3	15.82	-0.83	92.5	49.4		
WD 2117+539	11	3.3 ± 0.3	12.23	-0.57	95.8	53.2	0.50±0.03	1
WD 2136+828	10	-35.6 ± 0.4	5.21	-0.09	94.4	46.8	0.50±0.03	1
WD 2151−015	11	41.0 ± 0.7	14.97	-0.88	95.6	44.7		
WD 2151−015B	4	6.8 ± 3.9	5.09	-0.78	70.0	18.8		
WD 2226+061	10	40.7 ± 0.6	6.05	-0.13	92.2	40.8	0.43±0.03	1
WD 2341+322	5	7.5 ± 1.7	6.44	-0.77	84.5	22.7	0.57±0.03	5

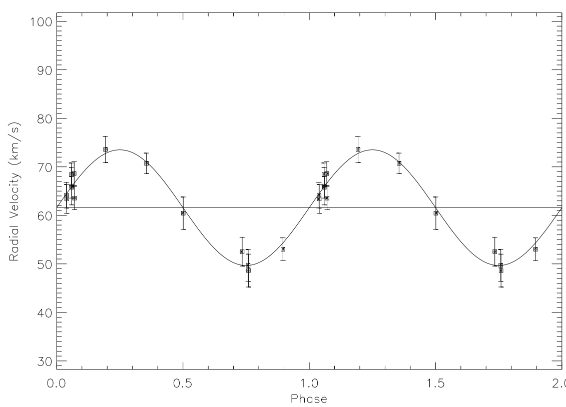

Figure 2. Measured radial velocities of WD 0101+048 and our best circular orbit fit (P=6.539d).

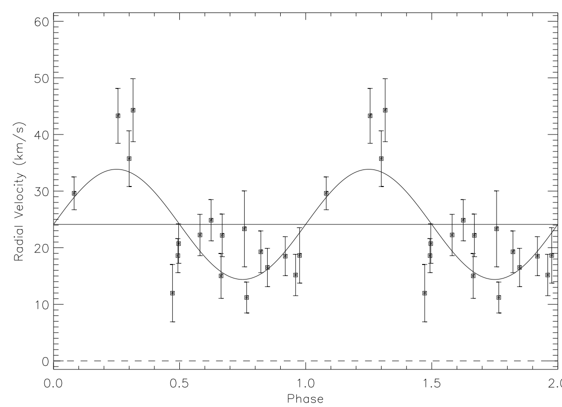

Figure 3. Measured radial velocities of WD 0416+701 and a circular orbit fit.

trials, so such a low value of chi-squared is to be expected occasionally given the number of binaries we have studied.

WD 0341+021: This star is clearly variable according to our criterion. The variability is due to an offset between two data sets (see Table 2). Although there is only one spectrum in the INT data set, the offset is clearly seen in the data and far exceeds the typical offset between data sets. We suspect this is a long period binary.

WD 0346−011: The Hα line of this star is weak and broad so we only used two Gaussians in the model line profile.

WD 0416+701: This star is certainly variable according to our criterion. We used the same procedure as for WD 0101+048 to re-calculate the model profile. There is a clear peak in the periodogram near 0.32d with no other significant peaks. A circular orbit fit to the measured radial velocities is given in Table 6. The χ^2 value for this fit is rather high so we present this as a tentative identification of the orbital period. The measured radial velocities and circular orbit fit are shown in Fig. 3

WD 0752−146: Schultz et al. (1992) found an emission line superimposed on the usual absorption line which shows variable radial velocity and indicates the presence of a companion. We measured the radial velocity of both the absorption and emission lines and found both to be slightly variable, though neither satisfies our strict criterion for binarity. The measurements of the emission line are listed in Tables 4 and 9 under WD 0752−146 B. We were unable to identify a definite period from our data combined with the data of Schultz et al.

WD 0945+245: This star, also known as LB 11146, was studied by Glenn et al. (1994) who found that the spectrum is a composite of a magnetic and a non-magnetic white dwarf. Their radial velocity measurements showed no variability over a baseline of 16 days. We find no evidence for variability from our own data nor from the combination of both sets of radial velocity measurements.

WD 0824+288: This is a rare DA+dC star (Finley et al. 1997) also known as PG 0824+289. We were unable to measure the radial velocity of the white dwarf from our 2 Hα spectra, but the results of measuring the radial velocity of the dC component measured from the Hα emission line are given in Tables 4 and 9 under WD 0824+288 B.

WD 1029+537: This hot white dwarf has a broad, shallow Hα line so we only used two Gaussians to form the model line profile.

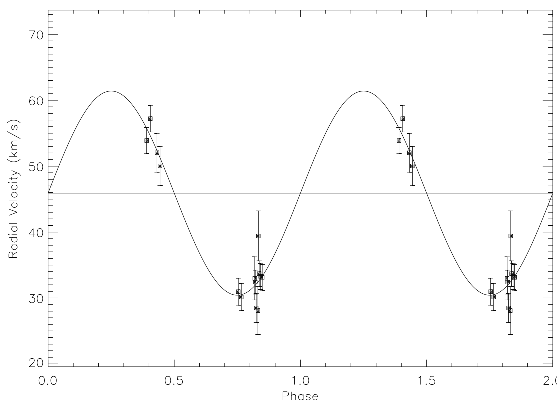

Figure 4. Measured radial velocities of WD 1407−475 and our circular orbit fit for a period near one day.

WD 1036+433: The core of the Hα line in star this reversed (in emission).

WD 1105−048: Although this star is variable according to our criterion, there are no obvious periods in the data and circular orbit fits to potential periods are not convincing. The uncertainties for several of the radial velocities given in Table 9 are very small. These uncertainties take no account of systematic errors in the data. If we assume there is an additional uncertainty of only 0.5 km s^{-1} in the data, we find $\log_{10}(p) = -3.3$. We believe that the data for this star simply reflect the fact that systematic errors in the data limit the accuracy of our radial velocity measurements to ≈ 0.5 km s^{-1}.

WD 1310+583: We only used data within 3500 km s^{-1} of Hα for the fitting process because four of our spectra only extend 3500 km s^{-1} to the red of Hα.

WD 1327−083: Although this star is variable according to our criterion, there are no obvious periods in the data and circular orbit fits to potential periods are not convincing. This would appear to be a similar case to WD 1105−048, i.e, the small uncertainties on some radial velocity measurements are over-optimistic.

WD 1407−475 This star is clearly variable according to our criterion. The variability is due to the large offset between two data sets (see Table 2). A periodogram shows significant peaks near 1, 2 and 3 cycles/d. We used the same technique applied to WD 0101+048 to measure the circular orbit fits to these three orbital periods given in Table 7. The fit for a period near one day is shown in Fig. 4. The circular orbit fits are good but further data is required to confirm this star is a binary and to then identify the correct orbital period.

WD 1615−157: This star incorrectly labelled as 1615−154 by Bragaglia et al. (1995) and Saffer, Livio & Yungelson (1998).

WD 2151−015: We found this star showed emission at Hα due to a companion which is variable in strength (Maxted et al. 1999). We used an additional Gaussian component to model the emission line, though it is not always visible in the spectra. Radial velocities for the 4 spectra where the line could be measured are listed in Tables 4 and 9 under WD 2151−015 B.

Table 5. Circular orbit fits to measured radial velocities of WD 0101+048. The uncertainty on the final digit of the period is given in parentheses.

Period (d)	HJD(T$_0$) −2451000	γ (km s^{-1})	K (km s^{-1})	χ^2
6.539(4)	3.9 ± 0.1	61.6 ± 1.1	11.9 ± 1.3	5.27
6.272(3)	0.3 ± 0.1	62.2 ± 0.7	12.1 ± 1.3	5.56
5.807(3)	5.7 ± 0.1	61.0 ± 0.8	10.9 ± 1.1	7.07
5.304(3)	5.9 ± 0.1	62.0 ± 1.0	11.8 ± 1.3	6.70
1.2093(2)	6.10 ± 0.03	62.3 ± 0.7	10.9 ± 1.1	6.49
1.1768(1)	6.65 ± 0.03	61.0 ± 0.8	10.7 ± 1.1	5.88
1.1461(1)	7.19 ± 0.03	59.1 ± 0.9	11.7 ± 1.3	7.02

Table 6. A circular orbit fit to the measured radial velocities of WD 0416+701. The uncertainty on the final digit of the period is given in parentheses.

Period (d)	HJD(T$_0$) −2451000	γ (km s^{-1})	K (km s^{-1})	χ^2
0.31854(2)	0.08 ± 0.01	24.9 ± 1.0	11.5 ± 1.6	30.0

5 DISCUSSION

5.1 Evidence for a population of single, low mass white dwarfs.

We have used the results in Table 4 to investigate whether there is any evidence for a population of single, LMWDs. For the purposes of this discussion we define an LMWD to be a white dwarf for which more than half the mass estimates, $M \pm \sigma_M$, satisfy the condition $(M_{\rm lim} - M) > 2\sigma_M$, i.e., they are at least two standard deviations below some mass limit $M_{\rm lim}$. The value of $M_{\rm lim}$ is a matter of some debate, so we consider three cases, $M_{\rm lim} = 0.45{\rm M}_{\odot}$,$M_{\rm lim} = 0.50{\rm M}_{\odot}$ and $M_{\rm lim} = 0.55{\rm M}_{\odot}$. Of the 20 white dwarfs which satisfy the condition $M_{\rm lim} = 0.55{\rm M}_{\odot}$, 19 show no evidence for a binary companion. The nature of the companion to WD 0341+021, if it is a binary, is not known. The results in Table 4 cannot be taken at face value because the obvious binaries have already been excluded. In order to account for these binaries we have reviewed our records to identify objects excluded from Table 4 which were observed because of their low mass and subsequently discovered to be binaries. There are 16 such stars, 3 of which have main-sequence companions and 13 of which are known or strongly suspected to have white dwarf companions.

It must be emphasized that we did not set out from the start to observe white dwarfs is such a way as to determine whether there is any evidence for a population of single LMWDs. The various stars were observed for different reasons, sometimes with a different motivation for the same star at different times. Nevertheless, these stars were, in general, observed because of their low mass and we continued to observe them if possible until we had either established

Table 7. Circular orbit fits to measured radial velocities of WD 1407−475. The uncertainty on the final digit of the period is given in parentheses.

Period (d)	HJD(T$_0$) −2450000	γ (km s^{-1})	K (km s^{-1})	χ^2
0.9985(3)	595.7 ± 0.1	46.2 ± 5.4	15.5 ± 5.2	10.7
0.50032(5)	595.10 ± 0.04	42.9 ± 1.4	12.8 ± 1.4	10.7
0.33320(1)	595.76 ± 0.02	41.8 ± 0.8	13.3 ± 0.9	11.9

an orbital period or had established that they were likely to be single. Therefore, our sample of LMWDS is fairly homogeneous and while it is not ideal it is, by far, the best available. We have simplified our analysis by assuming that there are only two populations of binary LMWDs, those with a companion of equal mass (population A) and those with companions of mass $0.08\mathrm{M}_{\odot}$ (population B) and that our detection efficiencies for these binaries are as given in Table 4. The question we address here is whether our data show evidence for a population of single LMWDs (population C). We then have two models. The first model is that all LMWDs belong to either population A or population B. We denote this model M2 because it contains only two populations. The second model is that there are three populations of LMWDs, A, B and C, so we denote this model M3. Using Bayes' theorem we find:

$$\frac{\mathrm{P(M3|D)}}{\mathrm{P(M2|D)}} = \frac{\mathrm{P(M3)}}{\mathrm{P(M2)}}\frac{\mathrm{P(D|M3)}}{\mathrm{P(D|M2)}},$$

where the usual notation applies, e.g., P(M2|D) is the probability of model M2 given our data, D. Our data consist of N_A LMWDs with white dwarf companions we identify as belonging to population A, N_B LMWDS with main-sequence companions we identify as belonging to population B and N_0 that are not detected as binaries. For these "non-detections", we have detection efficiencies $e_i(A)$ and $e_i(B)$, $i = 1, 2, \ldots, N_0$, for binaries belonging to population A and B, respectively. If some fraction f_A of binaries belong to population A and some fraction f_C of all LMWDs belong to population C, then

$$\frac{\mathrm{P(D|M3)}}{\mathrm{P(D|M2)}} = \frac{((1-f_C)f_A)^{N_A}((1-f_C)(1-f_A))^{N_B}\prod q_i}{f_A^{N_A}(1-f_A)^{N_B}\prod p_i}$$

where

$$p_i = f_A(1-e_i(A)) + (1-f_A)(1-e_i(B))$$

and

$$q_i = f_A(1-e_i(A)) + (1-f_A)(1-e_i(B)) + f_C$$

This ratio of probabilities has the considerable merit that we do not need to make any assumptions concerning the detection efficiencies for those LMWDs identified as belonging to population A or B. As we have no prior assumptions concerning the values of f_A or f_C, we simply integrate the function numerically over a uniform grid of all possible values. In addition, we can identify the most likely values of f_A and f_C given our data.

We have calculated the value of $\frac{P(D|M3)}{P(D|M2)}$ for the three cases shown in Table 8 corresponding to three different assumptions concerning the nature of the companion to WD 0341+021. We include the case of an undetected companion despite having noted this star as a binary to allow for this detection being a "false-alarm", though we consider this to be unlikely. Also given in Table 8 are the most likely values of f_A and f_C.

The sensitivity of our result to the assumed properties of just one star in a sample of 37 demonstrates that the results must be treated with some caution. However, they do seem to favour the existence of a population of single LMWDs. This result should not be taken as conclusive for several reasons. Firstly, we have assumed that some of the binaries from our other studies which show no sign of a companion star have white dwarf companions. If this is not the case, then the value $\frac{P(D|M3)}{P(D|M2)}$ may be much lower. Secondly, there have been many simplifying assumptions made concerning the nature of the companions to these star. Thirdly, we have used the theoretical period distribution for these binaries despite the problems with these theories. In summary, we can say the the data favour the existence of a population of single LMWDs, but this result is not conclusive.

Table 8. The ratio of probabilities $\frac{P(D|M3)}{P(D|M2)}$ for three different assumptions concerning WD 0341+021 and the most likely values of f_A and f_C and for three different uper limits to the mass, M_{lim}. The number of stars from Table 4 whose measured masses are two standard deviations below M_{lim}, N_{low}, is also given.

Companion to WD 0341+021	$\frac{P(D\|M3)}{P(D\|M2)}$	Model M2 f_A	Model M3 f_A	Model M3 f_C
M_{lim}=0.55M$_{\odot}$, N_{low} = 20				
Undetected	27	0.42	0.67	0.39
White dwarf	16	0.45	0.68	0.36
Main sequence	7	0.42	0.60	0.33
M_{lim}=0.50M$_{\odot}$, N_{low} = 14				
Undetected	48	0.49	0.68	0.30
White dwarf	30	0.52	0.70	0.27
Main sequence	17	0.48	0.62	0.23
M_{lim}=0.45M$_{\odot}$, N_{low} = 8				
Undetected	43	0.60	0.67	0.12
White dwarf	30	0.64	0.69	0.08
Main sequence	23	0.59	0.61	0.03

We have assumed that the companions to the LMWDs in our sample are either white dwarfs or main-sequence stars ($M \geq 0.08\mathrm{M}_{\odot}$). The question of whether companions of such low mass or lower (i.e., sub-stellar companions) can survive a common envelope phase is a difficult one to answer (Siess & Livio 1999). It would certainly be useful to continue observations of the LMWDs presented here to push down the limits on the mass of any possible companion.

5.2 Comparison with the results of Saffer, Livio & Yungelson (1998).

Several of the stars in this paper are candidate radial velocity variables from Saffer , Livio & Yungelson (1998). There are four "weight 1" candidates (WD 1232+479, WD 1310+583, WD 1647+591, WD 2117+539) and four "weight 2" candidates (WD 0401+250, WD 0549+158, WD 0839+231, WD 1229−012). Only one of these shows any hint of variability from our own data, which is quite extensive for all these stars. This is, perhaps, not surprising given that Maxted & Marsh (1999) found that the mean number of false detections of binaries expected in their survey based on the quoted uncertainty in the radial velocity measurements and the detection criterion is 17.7. This estimate is clearly too high given the number of binary candidates identified by the survey which were known to be binaries beforehand or which have been confirmed subsequently. This suggests that the typical uncertainty quoted for these radial velocity measurements is to low. It also shows the problems that can arise when trying to draw quantitative conclusions from a survey for binary stars based on rather subjective detection criteria.

6 CONCLUSION

We have presented 594 radial velocity measurements for 71 white dwarfs. We find that WD 0101+048 is certainly a binary, but are unable to determine whether the orbital period is near 6.4d or 1.2d. Similarly, WD 1407−475 is also a binary but we are unable to determine whether its orbital period is near 1d, 1/2d or 1/3d from our data. WD 0416+701 is likely to be binary and our data favours an orbital period of 0.32d, but further observations are required to show this convincingly. We also identify WD 0341+021 as another likely binary but are unable to establish the orbital period fom our data. There is some evidence in our data for a population of single, low mass white dwarfs, but this result is dependent on several assumptions.

ACKNOWLEDGEMENTS

PFLM was supported by a PPARC post-doctoral grant. CM was supported by a PPARC post-graduate studentship. The William Herschel Telescope and the Isaac Newton Telescope are operated on the island of La Palma by the Isaac Newton Group in the Spanish Observatorio del Roque de los Muchachos of the Instituto de Astrofisica de Canarias.

REFERENCES

Bergeron P., Saffer R.A., Liebert J., 1992, ApJ 394, 228.
Bergeron P., Liebert J., Fulbright M.S., 1995, ApJ 444, 810.
Bragaglia A., Renzini A., Bergeron P., 1995, ApJ 443, 735.
Finley D.S., Koester, D., Basri, G., 1997, ApJ 488, 375.
Glenn J., Liebert J, Schmidt G. 1994, PASP 106, 722.
Horne K., 1986, PASP 98, 609.
Homeier D., Koester D., Hagen H.-J., Jordan S., Heber U., Engels D., Reimers D., Dreizler S. ,1998, A&A 338, 563.
Iben I., Livio M., 1993, PASP 105, 1373.
Iben I., Tutukov A.V., Yungelson L. R., 1997, ApJ 475, 291.
Marsh, T.R., Dhillon, V.S., Duck, S.R., 1995, MNRAS 275, 828.
Maxted P.F.L., Marsh T.R., 1998, MNRAS 296, L34.
Maxted P.F.L., Marsh T.R., 1999, MNRAS 307, 122.
Maxted P.F.L., Marsh T.R.,Moran C.K.J., 2000, MNRAS, In press.
Moran C.K.J., Marsh T.R., Maxted P.F.L., 1999, In "11th European Workshop on White Dwarfs", Solheim J.-E. & Meištas E., eds., A.S.P. Conf. ser. Vol 169, p. 270.
Moran C.K.J., Maxted P.F.L., Marsh T.R., 2000, MNRAS, Submitted.
Moran, C.K.J., 1999, PhD thesis, University of Southampton.
Nelemans G., Tauris T.M, 1998, A&A 335, L85.
Saffer R.A., Livio M., Yungelson L.R., 1998, ApJ 502, 394.
Schultz, G., Zuckerman, B., Becklin, E.E, 1996, ApJ 460, 402.
Siess L., Livio M., 1999, 1999, MNRAS 304, 925.
Vennes S., Thejll P.A., Galvan R.G. et al., 1997, ApJ 480, 714.

Table 9. Measured heliocentric radial velocities.

Name	HJD -2400000	Radial velocity ($\mathrm{km\,s^{-1}}$)
EUVE1439+750		
	51241.6338	-144.2± 27.6
	51241.6998	-79.4± 25.6
	51242.7223	-170.4± 35.4
	51242.7370	-227.4± 36.2
HS1653+7753		
	51067.3966	-3.2± 11.1
	51067.4588	-0.8± 11.7
	51067.4730	-5.0± 11.0
	51243.6822	-4.9± 7.4
	51243.7039	4.0± 6.9
WD 0011+000		
	51071.5057	18.4± 5.7
	51071.5198	28.5± 3.6
	51071.6775	29.5± 4.0
WD 0101+048		
	50760.3534	49.7± 3.3
	50760.3606	48.6± 3.4
	50762.3176	68.4± 2.4
	50762.3271	65.8± 2.2
	50762.3885	68.6± 2.4
	50762.3957	63.5± 2.4
	51067.5292	52.5± 3.0
	51068.5837	53.0± 2.4
	51070.5287	73.6± 2.7
	51071.5898	70.7± 2.1
	51072.5427	60.4± 3.3
	50677.1806	64.2± 2.7
	50677.1879	63.4± 3.0
	50677.3150	66.0± 3.9
WD 0126+101		
	50777.4800	7.3± 1.8
	50777.4839	6.3± 1.9
	50777.5666	4.8± 2.2
	50777.5704	3.6± 2.3
	50778.5530	8.9± 1.4
	50778.5594	8.4± 1.9
WD 0132+254		
	50854.3391	34.1± 5.8
	50854.3603	25.8± 5.4
	50775.3529	36.3± 2.0
	50775.3696	36.4± 2.1
	50775.5094	38.2± 1.9
	50775.5260	37.2± 2.0
	50777.3592	34.6± 2.3
	50777.3737	36.1± 2.2
WD 0142+312		
	51067.5768	38.8± 7.3
	51067.5909	52.2± 5.3
	51067.6452	35.7± 14.9
	51067.6593	30.8± 9.9
	51067.7305	39.0± 5.9
	51068.5971	30.5± 4.8
	51068.6919	32.2± 5.1
	51069.7306	38.0± 4.9
WD 0143+216		
	51071.5352	27.6± 3.9
	51071.5493	13.7± 3.7
	51071.6594	22.7± 3.6
	51072.5870	19.8± 5.7
	51072.7436	18.0± 7.1

Table 9 – *continued*

Name	HJD -2400000	Radial velocity ($km\,s^{-1}$)
WD 0147+674		
	49742.3796	30.1± 4.7
	49742.3867	38.5± 4.7
	49742.3938	22.3± 4.7
	49739.3462	25.9± 5.2
	49739.3533	26.1± 6.1
	49739.3607	40.0± 6.1
WD 0148+467		
	51067.7424	14.1± 2.4
	51067.7495	16.4± 2.5
WD 0151+017		
	50778.5345	64.0± 2.2
	50778.5442	62.8± 2.2
	50778.6289	61.7± 2.6
	50778.6385	64.3± 2.7
WD 0213+396		
	51070.5847	56.6± 13.6
	51070.6694	22.8± 3.5
	51070.6835	27.2± 3.4
	51070.7341	19.9± 3.1
	51072.5191	54.3± 8.3
	51072.7257	28.9± 3.1
WD 0316+345		
	49742.4274	-43.6± 1.8
	49742.4333	-44.0± 1.8
	49742.4392	-44.2± 1.9
	49739.3721	-39.1± 2.0
	49739.3792	-45.2± 2.0
	49739.3863	-43.1± 2.1
	49738.4740	-41.0± 2.4
	49738.4870	-42.4± 2.7
	51067.6248	-43.6± 4.7
	51068.6430	-46.6± 2.6
	51068.6571	-48.2± 2.7
	51068.7065	-32.9± 2.6
WD 0320-539		
	50143.9069	61.3± 3.7
	50143.9254	63.7± 4.2
	50144.9013	52.1± 4.7
	50144.9197	44.3± 4.8
	50144.9387	64.4± 4.8
	50145.9028	55.8± 4.8
	50145.9212	58.9± 5.2
WD 0332+320		
	50778.5763	94.9± 4.5
	50778.5841	103.8± 4.4
	50778.6816	103.3± 5.8
	50778.6890	103.5± 5.9
WD 0339+523		
	49742.4503	5.8± 2.6
	49742.4601	4.4± 2.6
	49742.4695	-1.2± 2.6
	49739.4000	0.6± 3.4
	49739.4123	6.5± 2.8
	49739.4280	2.9± 2.8
	49739.4420	3.0± 2.9
	49738.5090	-2.2± 6.3
	49738.5237	7.3± 5.7
WD 0341+021		
	50855.3520	-22.3± 6.8
	50775.4488	-54.2± 2.1
	50775.4631	-53.6± 2.3
	50775.6270	-50.4± 2.4
	50775.6413	-49.3± 2.1
	50777.4505	-58.0± 2.2
	50777.4649	-57.3± 2.3
WD 0346-011		
	51068.7409	89.6± 35.2
	51069.7458	70.4± 43.9
	51070.7131	99.8± 55.2
	51070.7202	179.9± 54.6
	51071.6169	42.2± 47.1
	51071.6240	310.4± 46.0
	51071.6871	120.5± 43.6
	51071.6942	121.1± 43.0
	51071.7517	225.3± 48.7
	51071.7589	136.0± 51.5
WD 0401+250		
	50855.3979	83.4± 3.1
	50855.4052	80.1± 3.3
	50760.6725	85.2± 3.5
	50760.6844	83.4± 3.4
	50762.7069	84.6± 2.3
	50762.7147	79.3± 3.0
	50778.5921	80.9± 3.0
	50778.5948	75.5± 2.9
	50778.5977	84.3± 2.9
	50778.7358	79.0± 3.2
	50778.7397	81.6± 3.3
WD 0407+179		
	51243.3924	62.5± 2.3
WD 0416+334		
	50775.5542	-43.8± 2.1
	50775.5638	-43.4± 2.3
	50776.7101	-43.4± 4.5
	50776.7198	-50.7± 4.6
	50777.6938	-50.9± 3.1
	50777.7058	-40.7± 2.5
WD 0416+701		
	51067.6951	43.9± 4.6
	51067.7092	36.1± 4.7
	51068.5631	18.6± 4.6
	51068.6714	44.1± 5.3
	51068.7214	11.7± 4.8
	51070.6974	15.3± 3.8
	51070.7477	19.4± 3.5
	51071.6010	21.0± 3.3
	51071.7360	18.6± 3.3
	51072.6416	24.0± 6.4
	51072.7064	15.2± 3.5
	51240.4325	22.3± 3.5
	51240.4466	25.0± 3.4
	51240.4606	22.3± 3.6
	51241.4751	16.1± 3.2
	51242.4061	11.3± 2.6
	51243.4642	29.6± 2.8
	51271.3573	18.6± 2.8

Table 9 – *continued*

Name	HJD -2400000	Radial velocity (km s^{-1})
WD 0437+152		
	50854.3885	20.1± 5.0
	50854.4097	22.6± 3.3
	50775.5751	20.9± 2.5
	50775.5917	19.0± 2.7
	50777.5226	22.1± 2.4
	50777.5368	24.9± 2.5
	50777.6274	15.5± 3.2
	50777.6417	20.9± 3.6
WD 0446-789		
	50143.9414	42.7± 2.6
	50143.9470	38.6± 2.4
	50144.9550	39.3± 2.7
	50144.9623	40.5± 3.0
	50145.9372	37.9± 2.6
	50145.9446	40.4± 2.4
	50145.9519	42.6± 2.6
WD 0453+418		
	49742.4820	57.5± 1.7
	49742.4879	56.9± 1.6
	49742.4939	60.0± 1.6
	49742.5007	57.8± 1.6
	49739.4570	59.4± 1.6
	49739.4641	60.0± 1.8
	49739.4712	59.9± 1.7
	49738.5463	60.5± 3.4
	49738.5572	61.6± 2.7
	51238.3489	52.0± 4.1
	51238.4277	62.6± 4.9
	51238.4936	52.4± 8.9
	51240.3560	59.2± 2.0
	51241.3672	62.9± 2.0
	51242.4281	67.2± 1.9
WD 0507+045.1		
	50775.6142	36.6± 2.9
	50775.6181	36.3± 3.1
	50776.7292	33.7± 4.8
	50776.7366	35.2± 5.5
	50777.5554	45.9± 3.5
	50777.5593	36.6± 3.3
WD 0507+045.2		
	50775.6142	43.4± 4.9
	50775.6181	47.0± 5.2
	50776.7292	59.6± 9.2
	50776.7366	49.3± 10.9
	50777.5554	44.7± 6.1
	50777.5593	55.1± 5.9
WD 0509-007		
	51240.4144	24.2± 3.7
	51240.4959	18.0± 10.8
	51241.4268	26.1± 3.8
	51242.3366	15.9± 5.1
	51242.4480	20.8± 3.1
WD 0516+365		
	50778.6086	52.7± 4.6
	50778.6160	57.0± 4.6

Table 9 – *continued*

Name	HJD -2400000	Radial velocity (km s^{-1})
WD 0549+158		
	50852.3862	29.7± 4.9
	50852.3969	28.3± 4.1
	50852.4088	35.4± 4.7
	50852.5026	19.7± 5.5
	50852.5099	38.8± 8.2
	50852.5138	35.3± 7.9
	50854.4282	22.9± 6.4
	50854.4320	41.9± 6.3
	50854.4358	19.2± 6.3
	50855.3795	44.0± 26.2
	50855.3868	26.5± 6.7
	51238.4681	24.4± 10.2
	51238.4787	41.8± 13.5
	51240.3339	34.4± 6.4
	51240.3411	37.4± 6.3
	51241.3499	30.3± 4.2
	51243.4199	27.9± 4.6
WD 0658+624		
	50775.6884	11.9± 3.5
	50775.7015	9.9± 3.0
	50776.7544	22.9± 4.9
	50776.7710	16.3± 3.5
	50777.7215	14.4± 2.8
	50777.7359	12.1± 3.1
WD 0752-146		
	51243.3630	30.7± 4.1
	51243.3717	26.2± 4.0
	51243.4397	21.6± 2.7
	51267.8694	40.4± 3.5
WD 0752-146B		
	51243.3630	-152.2± 4.3
	51243.3717	-158.6± 4.2
	51243.4397	-138.9± 2.8
	51267.8694	-147.6± 3.7
WD 0808+595		
	50852.5339	3.5± 8.3
	50852.5559	32.7± 8.7
	50775.7134	14.7± 5.3
	50775.7300	9.8± 7.4
	50777.5917	18.2± 6.1
	50777.6060	19.8± 6.7
	50777.7610	12.6± 4.7
WD 0824+288B		
	50777.7806	-36.5± 3.0
	50777.7846	-37.1± 2.7
WD 0839+231		
	49742.5339	-2.1± 3.5
	49742.5398	-1.7± 3.5
	49742.5457	1.1± 3.6
	49739.5844	2.9± 3.4
	49739.5916	-0.1± 3.6
	49739.5987	-0.8± 3.4
	49738.6393	-1.1± 3.0
	49738.6501	5.8± 3.9
WD 0906+296		
	50775.6573	94.2± 3.3
	50775.6670	90.8± 3.9
	50775.7501	111.4± 11.1
	50775.7622	96.1± 8.3
	50775.7744	93.8± 4.0
	50775.7864	93.5± 7.9
	50777.6576	93.8± 5.6
	50777.6673	86.5± 8.1

Table 9 – *continued*

Name	HJD -2400000	Radial velocity ($km\,s^{-1}$)
WD 0913+442		
	50760.7469	57.2± 3.0
	50760.7645	57.4± 3.1
	50761.6966	62.8± 3.7
	50761.7119	53.3± 3.9
	50762.7240	63.2± 3.1
	50762.7393	57.2± 3.1
WD 0945+245		
	51240.4008	67.7± 9.5
	51241.4105	70.9± 7.1
	51242.3625	58.1± 8.4
	51242.6266	56.0± 8.0
	51243.4934	59.1± 8.4
WD 0950-572		
	51267.8817	46.8± 6.8
	51267.8958	45.7± 6.6
WD 0954+247		
	50761.7309	56.2± 2.6
	50762.6712	56.8± 2.9
	50762.6853	59.3± 2.9
	50762.7556	64.5± 2.6
	50762.7692	62.3± 2.7
WD 0954-710		
	50143.0878	24.6± 2.6
	50143.0998	23.4± 1.7
	50144.1095	18.3± 1.7
	50145.0226	17.7± 1.5
	50145.0300	17.0± 1.5
	50146.1061	16.8± 1.4
	50146.1134	17.9± 1.4
WD 1026+023		
	50776.7813	26.4± 4.4
	50776.7851	28.5± 4.4
	50776.7890	15.8± 4.7
	50777.7908	16.9± 2.4
	50777.7947	14.9± 3.4
	50778.6587	16.7± 3.2
	50778.6627	16.3± 3.1
	50778.7867	18.9± 4.7
WD 1029+537		
	51004.3892	13.2± 23.6
	51241.4523	-19.6± 23.3
	51242.5058	54.9± 19.9
	51242.5274	79.7± 20.1
	51243.5192	24.7± 24.5
WD 1031-114		
	51238.5873	44.9± 6.4
	51238.6013	35.2± 4.8
	51241.5576	43.3± 2.8
	51241.5682	40.6± 2.7
	51242.5494	39.0± 2.3
	51243.5883	40.3± 2.7
	51267.9177	57.7± 15.1
	51268.0079	43.4± 2.4
WD 1036+433		
	49162.3636	-7.1± 1.5
	49162.3692	-6.1± 1.4
	49153.3770	-4.9± 1.9
	49153.3815	-4.3± 1.8
	49150.3969	-4.8± 1.4

Table 9 – *continued*

Name	HJD -2400000	Radial velocity ($km\,s^{-1}$)
WD 1039+747		
	49742.5553	34.0± 9.9
	49742.5659	56.0± 9.6
	49739.6153	52.5± 12.6
	49739.6259	51.0± 12.6
WD 1105-048		
	51241.5141	50.4± 1.6
	51241.5247	48.3± 1.3
	51241.6078	50.7± 1.6
	51241.6184	49.8± 1.5
	51241.7391	56.2± 4.2
	51242.6453	52.1± 1.6
	50527.1917	50.4± 1.3
	50527.1991	50.0± 1.5
	50528.1782	57.1± 2.8
	50528.1925	49.8± 1.5
	50143.1897	53.3± 1.3
	50143.1947	53.3± 0.3
	50144.1248	51.0± 1.6
	50144.1309	50.7± 1.2
	50145.1577	50.7± 0.3
	50145.1627	50.6± 0.4
	50146.1267	48.9± 0.8
	50146.1318	49.4± 0.3
WD 1229-012		
	51238.6209	27.8± 6.5
	51238.6349	14.9± 9.4
	51238.7430	-27.9± 13.3
	51238.7571	31.5± 11.5
	51240.6630	23.7± 3.7
	51240.7640	5.5± 5.3
	51243.6141	15.4± 3.4
	51268.0433	21.6± 3.6
	51268.1519	25.6± 7.4
WD 1232+479		
	50852.7120	-6.6± 5.0
	50852.7333	2.4± 3.2
	50853.6397	9.5± 2.8
	50853.6488	7.5± 4.2
	50853.7267	9.0± 3.9
	50853.7339	8.1± 3.9
	50854.5369	0.9± 2.8
	50854.5501	3.6± 3.1
	50854.6129	9.5± 3.1
	50854.6248	9.8± 2.8
WD 1257+032		
	49888.4357	34.3± 5.2
	49888.4578	21.5± 5.3
	49889.4251	28.4± 4.1
	49889.4471	12.9± 4.4
	49891.4325	25.0± 5.1
	49891.4551	25.0± 4.7
	49892.3956	22.4± 6.1
	49892.4290	4.5± 6.6
	49893.4011	25.3± 7.7
	49893.4230	18.9± 7.3
	49742.7052	24.4± 3.4
	49742.7157	28.6± 3.2
	49742.7279	24.4± 3.2
	51243.6395	14.4± 8.6
	51268.0664	26.6± 9.4
	51268.1739	14.9± 8.6
	51268.1880	31.6± 10.1

Table 9 – *continued*

Name	HJD -2400000	Radial velocity ($km\,s^{-1}$)
WD 1310+583		
	50852.7572	5.9± 3.3
	50852.7679	8.8± 5.2
	50852.7753	3.1± 6.0
	50853.6595	-3.3± 5.9
	50853.6658	7.2± 5.1
	50853.7830	3.5± 3.9
	50853.7902	4.1± 3.8
	50854.5618	-1.4± 4.5
	50854.5691	-4.7± 6.5
	50854.6392	4.1± 3.8
	50854.6465	8.7± 3.9
	50622.4786	5.6± 3.1
	50622.4937	2.8± 3.8
	50623.4525	7.7± 3.9
	50623.4667	5.1± 3.7
WD 1327-083		
	50967.9597	43.9± 1.5
	50967.9654	43.2± 1.0
	50968.0884	44.5± 1.2
	50968.8552	44.7± 0.2
	50969.8352	46.0± 0.9
	50526.1851	44.0± 0.8
	50526.1902	45.6± 0.8
	50527.2171	44.6± 1.1
	50527.2222	44.7± 1.1
	50528.2536	42.9± 0.3
	50143.2033	43.3± 0.4
	50143.2072	43.2± 0.3
	50144.1877	47.8± 0.3
	50144.1904	42.7± 1.5
	50145.1993	46.2± 0.4
	50145.2026	46.4± 0.3
	50145.2065	46.5± 0.3
	50146.1930	43.2± 1.1
	50146.1969	46.0± 0.2
WD 1353+409		
	49739.7582	6.7± 5.4
	49739.7688	7.6± 5.1
	49739.7794	-7.7± 6.1
	49739.7918	3.4± 5.4
	49162.4427	-2.4± 4.4
	49162.4602	-4.0± 4.7
	49153.4798	3.7± 9.9
	49153.5087	-1.9± 12.9
	49150.5101	5.3± 5.8
	49150.5212	-0.1± 5.8
	49150.5349	0.6± 5.5
	50860.6645	-5.2± 2.7
	50860.6933	-6.5± 2.1

Table 9 – *continued*

Name	HJD -2400000	Radial velocity ($km\,s^{-1}$)
WD 1407-475		
	50526.2013	53.9± 2.0
	50526.2159	57.2± 2.0
	50527.2527	50.0± 3.0
	50527.2407	52.0± 2.9
	50143.2263	28.5± 2.2
	50143.2439	33.3± 2.0
	50144.1538	31.0± 2.0
	50144.1658	30.1± 2.0
	50144.2366	33.7± 1.9
	50144.2486	33.1± 1.9
	50145.2174	33.0± 3.3
	50145.2317	39.4± 3.8
	50146.2179	32.4± 1.8
	50146.2284	28.1± 3.6
WD 1422+095		
	50143.2637	4.9± 2.9
	50144.1992	2.4± 2.3
	50144.2111	0.1± 2.2
	50145.2508	-2.8± 5.0
	50145.2650	-10.2± 4.1
	50146.2722	7.6± 3.0
WD 1507+220		
	49888.4890	-53.3± 4.2
	49888.5122	-50.4± 4.0
	49889.4840	-52.0± 3.7
	49889.5027	-47.6± 3.7
	49891.4837	-48.1± 3.9
	49891.5024	-45.0± 3.8
	49892.4597	-54.6± 4.5
	49892.4781	-55.8± 4.4
	49893.4511	-54.1± 6.1
	49893.4694	-51.6± 5.9
WD 1507-105		
	51268.2383	-14.1± 4.5
	51268.2525	-13.6± 6.6
WD 1614+136		
	49155.6365	2.0± 4.8
	49155.6561	4.3± 7.8
	49162.4850	7.3± 4.8
	49162.4963	17.9± 4.6
	49162.5935	11.7± 4.5
	49162.6049	0.5± 4.7
	49153.5447	17.9± 12.3
	49153.5635	-1.5± 10.3
	49153.5797	35.5± 15.3
	49150.5559	-4.9± 4.0
	49150.5669	10.8± 4.1
	50860.7205	3.8± 1.8
	50860.7494	4.4± 2.5
	50860.7730	6.2± 3.7
	50969.0777	4.6± 4.5
WD 1615-157		
	50528.2252	10.8± 7.3
	50528.2361	14.2± 6.0

Table 9 – *continued*

Name	HJD -2400000	Radial velocity ($km\,s^{-1}$)
WD 1620-391		
	50676.8555	45.3± 0.9
	50676.8593	46.6± 0.9
	50676.8631	47.0± 0.9
	50677.0418	44.9± 2.0
	50677.0435	44.6± 2.1
	50677.8541	47.6± 1.1
	50968.0006	47.1± 1.5
	50528.2034	48.5± 1.4
	50528.2115	47.6± 1.6
	50528.2972	50.8± 1.1
	50528.3052	51.1± 1.1
WD 1637+335		
	51071.3364	29.6± 4.6
	51071.3505	34.4± 3.4
	51071.4081	20.0± 3.8
	51072.3472	25.4± 3.9
	51072.4038	26.5± 3.9
WD 1647+591		
	51067.3415	48.4± 3.7
	51067.3460	40.4± 3.8
	51067.4252	41.4± 3.9
	51067.4289	41.6± 3.8
	51068.3308	42.0± 6.2
	51068.3345	40.2± 5.1
	51068.3382	43.8± 4.9
	51068.4093	40.2± 3.5
	51069.3372	42.2± 10.5
	51069.3483	27.0± 22.4
	51069.4029	39.2± 5.9
	51071.3235	61.4± 38.4
	51071.3260	30.0± 6.8
WD 1655+215		
	51067.3588	43.1± 3.2
	51067.4136	37.9± 3.3
	51068.3483	42.6± 4.7
	51068.3589	32.1± 4.6
	51072.4521	50.9± 8.1
WD 1911+135		
	49888.5600	23.6± 3.3
	49888.5684	16.8± 3.2
	49889.5480	26.8± 3.1
	49889.5564	23.3± 3.0
	49891.5509	23.1± 4.1
	49891.5589	20.5± 3.9
	49892.5223	18.6± 3.8
	49892.5303	15.3± 3.7
	49893.5143	19.0± 5.2
	49893.5234	12.3± 5.2
WD 1943+163		
	49888.5912	36.3± 3.7
	49888.6003	39.0± 3.9
	49889.5695	33.6± 4.0
	49889.5778	35.8± 4.4
	49891.5725	42.8± 5.0
	49891.5804	40.0± 4.9
	49892.5447	30.5± 4.6
	49892.5527	34.8± 4.8
	49893.5403	40.1± 6.9
	49893.5494	40.7± 8.2
	50969.1790	34.6± 4.4
	50969.1863	35.0± 4.3
	50970.1076	35.6± 2.5
	50970.2356	36.8± 2.2

Table 9 – *continued*

Name	HJD -2400000	Radial velocity ($km\,s^{-1}$)
WD 2058+506		
	51067.5098	12.5± 6.0
	51067.5437	10.4± 6.0
	51067.5578	18.4± 6.7
	51067.6074	10.0± 10.5
	51068.5067	11.0± 15.6
	51068.6129	13.1± 6.0
	51068.6270	4.8± 5.2
	51070.5105	-6.3± 7.0
	51070.5574	6.3± 4.2
	51071.4598	-2.1± 5.0
	51071.4704	5.8± 4.6
	51071.5634	9.8± 5.1
	51071.5741	12.6± 4.9
	51071.6386	8.0± 4.6
	51072.4717	22.5± 7.5
WD 2111+261		
	50759.3525	7.6± 4.8
	50759.3649	1.9± 4.1
	50760.3017	-3.4± 3.3
	50760.3124	-3.3± 3.4
	50760.3707	-2.4± 2.9
	50760.3814	-2.1± 2.6
	50761.3014	-7.5± 2.7
	50761.3121	-4.4± 2.8
	50761.3627	1.1± 2.6
	50761.3734	-1.9± 2.6
	50762.3365	-7.0± 2.7
	50762.3471	0.5± 2.4
WD 2117+539		
	49888.6092	4.2± 3.4
	49888.6119	5.4± 3.5
	49888.6166	5.1± 2.0
	49889.5864	6.6± 2.4
	49889.5909	2.7± 2.5
	49891.5950	3.8± 2.4
	49891.5995	3.4± 2.2
	49892.5617	0.5± 2.5
	49892.5662	-3.5± 2.5
	49893.5595	3.0± 3.2
	49893.5646	5.6± 3.2
WD 2136+828		
	49888.6248	-31.8± 3.2
	49888.6297	-34.6± 3.1
	49889.5988	-35.5± 3.2
	49889.6033	-37.7± 3.3
	49891.6085	-36.4± 2.9
	49891.6130	-33.6± 2.9
	49892.5743	-34.7± 3.7
	49892.5788	-41.2± 3.6
	49893.5734	-38.1± 5.0
	49893.5779	-35.5± 5.6
WD 2151-015		
	51068.5265	44.4± 9.6
	51068.5265	46.4± 7.7
	51069.5395	49.3± 9.3
	51070.5434	31.6± 5.6
	51071.4883	39.4± 6.1
	51072.4986	25.0± 7.8
	50675.9728	39.4± 3.9
	50676.1780	43.9± 3.4
	50676.1888	38.4± 3.6
	50677.2607	34.6± 10.2
	50968.2692	50.4± 4.3

Table 9 – *continued*

Name	HJD -2400000	Radial velocity ($km\,s^{-1}$)
WD 2151-015B		
	50676.1780	-5.7± 10.2
	50676.1888	-6.1± 12.8
	50677.2607	7.5± 2.5
	50968.2692	33.3± 16.8
WD 2226+061		
	49888.6498	43.9± 4.2
	49888.6654	42.7± 4.0
	49889.6551	37.4± 4.0
	49889.6706	38.7± 4.3
	49891.6345	42.8± 4.4
	49891.6494	43.8± 4.5
	49892.5989	40.9± 5.4
	49892.6138	34.8± 5.1
	49893.5987	32.2± 8.0
	49893.6137	49.5± 8.3
WD 2341+322		
	51067.6780	-1.1± 4.2
	51067.6852	10.1± 10.6
	51068.5421	9.3± 2.6
	51068.5528	8.7± 2.0
	51069.5867	-4.3± 10.2